Available online at www.sciencedirect.com

ScienceDirect

Nuclear Physics B 967 (2021) 115432

NUCLEAR PHYSICS B

www.elsevier.com/locate/nuclphysb

Probing four-fermion operators in the triple top production at future hadron colliders

Sara Khatibi [a,*], Hamzeh Khanpour [b,c,d]

[a] *Department of Physics, University of Tehran, North Karegar Ave., Tehran 14395-547, Iran*
[b] *Department of Physics, University of Science and Technology of Mazandaran, P.O. Box 48518-78195, Behshahr, Iran*
[c] *School of Particles and Accelerators, Institute for Research in Fundamental Sciences (IPM), P.O. Box 19395-5531, Tehran, Iran*
[d] *Department of Theoretical Physics, Maynooth University, Maynooth, Co. Kildare, Ireland*

Received 23 March 2021; received in revised form 2 May 2021; accepted 4 May 2021
Available online 10 May 2021
Editor: Tommy Ohlsson

Abstract

In this paper, we study the triple top quark production at the future high-energy proton-proton colliders to probe the four-fermion interactions involving three top quarks. We employ the Standard Model Effective Field Theory (SMEFT) to find the upper limits at 95% CL on the Wilson coefficients of these kinds of four-fermion operators. We consider a detailed analysis with a unique signal signature of two same-sign leptons. A full simulation chain includes all the relevant backgrounds, realistic detector simulations, and a cut-based technique are taken into account. This study is presented for the HE-LHC working at the center of mass energy of 27 TeV with 15 ab^{-1} and FCC-hh working at the center of mass energy of 100 TeV with 30 ab^{-1}. We show that the future high-energy proton-proton colliders could reach an impressive sensitivity to four-fermion contact interactions involving three top quarks.

1. Introduction

All experimental measurements agree well with the Standard Model (SM) forecasts so far. It suggests that the scale of new physics is much above the electroweak scale and these two scales

* Corresponding author.
E-mail addresses: Sara.Khatibi@ut.ac.ir (S. Khatibi), Hamzeh.Khanpour@cern.ch (H. Khanpour).

https://doi.org/10.1016/j.nuclphysb.2021.115432

are well separated from each other. In other words, the new heavy degrees of freedom cannot be produced directly in the experiments, however, they can affect the SM couplings or induce the new interaction between the SM degrees of freedom.

The Standard Model Effective Field Theory (SMEFT) provides a framework for studying the effect of new physics [1]. The SMEFT Lagrangian only contains the SM particles and respects the Lorentz and the SM gauge symmetry, i.e. SU(3)×SU(2)×U(1). In this framework, the new degrees of freedom are integrated out and their effects show up as the new interaction between the SM particles in the form of higher dimension operators in the Lagrangian. The higher dimensional terms are proportional to the inverse powers of the scale of new physics. Assuming baryon number conservation, the leading corrections to the SM interactions come from one dimension-five and 59 dimension-six independent operators [2].

Being a model-independent approach is one of the advantages of the SMEFT framework since the various new physics scenarios exist in the market which sometimes have the same signatures in the experiment environments. Hence, one can use this model-independent framework and find the experimental values or limits on the Wilson coefficients of higher-dimensional operators and then translate them to the matching couplings of any new physics model. Among dimension-6 operators, four-fermion contact interaction can be originated at tree level in the UV models so they can have large Wilson coefficients [3]. There are several papers in the literature that has studied the four-fermion interactions using different observables. In Ref. [4], the dijet measurements at the Large Hadron Collider (LHC) have been utilized to search for four-light quark operators. In addition, the four-lepton contact interactions have been considered in Ref. [5,6].

Due to the interesting properties of top quark, studying the four-fermion operators involving the top quark is also important. Ref. [7] constrained the four-top quark operators by studying the $t\bar{t}b\bar{b}$ signature at the LHC. Furthermore, single and pair top quark production data is used for finding the bounds on the four-top quark coefficients [8,9]. Moreover, four-top quark production has been utilized to probe four-top quark operators [9–11]. The ATLAS collaboration has searched for four-top quark production at $\sqrt{s} = 8$ TeV to probe four-top quark contact interactions [12,13]. The two top-two light quark and two top-two lepton operators have been studied in top pair production in the hadron and lepton colliders in Ref. [14]. Also, the effect of four-fermion operators involving only one top quark in single top production and top decay width has been considered in this paper as well. Ref. [15,16] have provided a comprehensive global analysis using the top quark LHC data to probe four-quark operators including two top-two light quark operator. The effect of the one top-light quarks operators on the polarization of single top quarks in the t-channel process at the LHC has been studied in Ref. [17]. Moreover, by using the result of LHC searches for rare top decay $t \to Zj$, bounds on the operators involving one top-one light quark-leptons has been determined in Ref. [18–20].

However, the four-fermion operators with three top and one light quarks have not received more attention, since hardly any experimental observables are sensitive to these operators [21]. In this paper, we explore this kind of four-fermion operators in three top quarks and three top quarks+jet productions in hadron colliders. The cross-section production of the triple top quarks at the hadron collider is small compared with other top quark production channels in the SM framework [22]. The reason for this relatively small cross-section is the existence of b-quark in the initial state (most of the time) and the weak couplings in these processes. Since the beyond SM models can enhance the rate of triple top quark production, this signature can be valuable to show the effect of the new physics.

Previously, the triple top production has been considered for exploring some beyond SM models [22–25]. For example in Ref. [26,27], authors utilized the three top production for constraining the top quark flavor changing neutral couplings (FCNC) with the gluon, Higgs and Z boson, and photon. Moreover, this signature has been considered in Refs. [28] and [29] for probing the contact interactions at the LHC with 13 and 14 TeV center-of-mass energies.

In this study, we consider a full set of four-fermion operators involving three top quarks. A detailed analysis is performed for the triple top production to probe this kind of contact interaction at the high energy LHC (HE-LHC) [30,31] and the Future Circular Collider (FCC-hh) [32] with integrated luminosity of 15 ab^{-1} and 30 ab^{-1}, respectively. The unique signature of two same-sign leptons final state is taken into account in order to suppress the SM backgrounds. By considering the signal scenario, we consider all the relevant background processes which have similar final state topology. Furthermore, parton showering and hadronization as well as the realistic detector simulations are taken into consideration. Although our aim here is probing the Wilson coefficients of four-fermion operators involving three top quarks in triple tops production, finally we constrain the parameters of the UV complete model containing a leptophobic gauge boson Z' by using the limits on the Wilson coefficients.

The rest of the paper is organized as follows. The theoretical framework considered in this study is introduced in section 2. The details of our analysis strategy is presented in section 3. The sensitivity of the future high energy hadron colliers to the Wilson coefficients of four-fermion operators involving the three top quarks appear in section 4. Finally, the summary of the paper is presented in section 5.

2. Theoretical formalism

In this section, we introduce the operators involving three top and light quarks in the context of the SMEFT. All the new degrees of freedom are integrated out in this framework and their effects are encoded in the new interaction between the SM fields with the appearance of the higher dimensional operators in the Lagrangian. These effective operators respect the Lorentz and SM gauge symmetries. By considering the baryon and lepton conservation, the SMEFT Lagrangian up to the dimension-six operators are written as follows,

$$\mathcal{L}_{\rm SMEFT} = \mathcal{L}_{\rm SM} + \sum_i \frac{C_i O_i}{\Lambda^2}, \tag{1}$$

where the first term is the SM Lagrangian containing dimension-four operators. The dimension-six operators and their corresponding coefficients are shown by O_i and C_i, respectively. The scale of new physics is indicated by Λ. Among the four-fermion contact interactions, following operators could generate the interaction terms between three top and one light quarks [2,33],

$$\begin{aligned}
O_{qq}^{1(ijkl)} &= \left(\bar{q}_i\gamma^\mu q_j\right)\left(\bar{q}_k\gamma_\mu q_l\right), \\
O_{qq}^{3(ijkl)} &= \left(\bar{q}_i\gamma^\mu \tau^I q_j\right)\left(\bar{q}_k\gamma_\mu \tau^I q_l\right), \\
O_{uu}^{(ijkl)} &= \left(\bar{u}_i\gamma^\mu u_j\right)\left(\bar{u}_k\gamma_\mu u_l\right), \\
O_{qu}^{1(ijkl)} &= \left(\bar{q}_i\gamma^\mu q_j\right)\left(\bar{u}_k\gamma_\mu u_l\right), \\
O_{qu}^{8(ijkl)} &= \left(\bar{q}_i\gamma^\mu T^A q_j\right)\left(\bar{u}_k\gamma_\mu T^A u_l\right),
\end{aligned} \tag{2}$$

where q and u indicate the left-handed quark doublet and right-handed quark singlet, respectively, and i, j, k, l are flavor indices. The Pauli matrices are shown by τ^I and $T^A = \lambda^A/2$ where

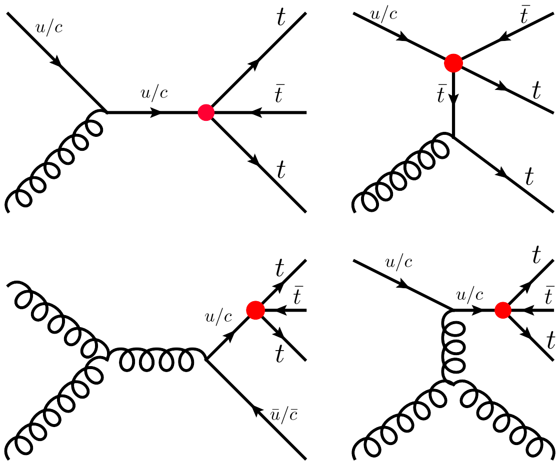

Fig. 1. Representative Feynman diagrams for the signal. The triple top and triple top in association with a jet production in presence of the four-fermion contact interactions are shown in the first row and second row, respectively.

λ^A are Gell-Mann matrices. The relevant effective Lagrangian, containing interaction between three top quarks and one light quark, is obtained as follows,

$$\begin{aligned}\mathcal{L}_{\rm eff} = \frac{1}{\Lambda^2}[& C_{qq_u}(\bar{t}_L\gamma^\mu t_L)(\bar{t}_L\gamma_\mu u_L) + C_{uu}(\bar{t}_R\gamma^\mu t_R)(\bar{t}_R\gamma_\mu u_R) \\ & + C_{qu_R}(\bar{t}_L\gamma^\mu t_L)(\bar{t}_R\gamma_\mu u_R) + C_{qu_L}(\bar{t}_R\gamma^\mu t_R)(\bar{t}_L\gamma_\mu u_L) \\ & + C_{qq_c}(\bar{t}_L\gamma^\mu t_L)(\bar{t}_L\gamma_\mu c_L) + C_{cc}(\bar{t}_R\gamma^\mu t_R)(\bar{t}_R\gamma_\mu c_R) \\ & + C_{qc_R}(\bar{t}_L\gamma^\mu t_L)(\bar{t}_R\gamma_\mu c_R) + C_{qc_L}(\bar{t}_R\gamma^\mu t_R)(\bar{t}_L\gamma_\mu c_L)] \\ & + h.c. \end{aligned} \tag{3}$$

In this study, we consider operators containing the u-quark and c-quark separately. In the next section, the above effective Lagrangian is employed to study the triple top quark production at the future high energy hadron colliders to probe the four-fermion operators.

3. Analysis strategy

In this section, we present our signal and the related SM background processes. We also describe in details the event generation and simulation method. As mentioned before, we are interested in the triple top quark production (+jet) at the future hadron collider to search for the four-fermion contact interactions. We perform the analysis for the HE-LHC and FCC-hh working at the center of mass energies of $\sqrt{s} = 27$ TeV and $\sqrt{s} = 100$ TeV, respectively.

The signal process is three top quarks production where two same-sign top quarks decay leptonically and the other one decay hadronically. We also add three top quarks production in association with a jet to the signal process. Consequently, the final state consists of two same-sign charged leptons (electron or muon), three b-jets, two or three light-jets, and missing energy due to the presence of the neutrino:

$$pp \to tt\bar{t}(+j) \to \ell^+\ell^+ + 3\text{ b-jet} + 2(+1)\text{ light-jet} + \not{E}_T\,,$$
$$pp \to \bar{t}\bar{t}t(+j) \to \ell^-\ell^- + 3\text{ b-jet} + 2(+1)\text{ light-jet} + \not{E}_T\,.$$

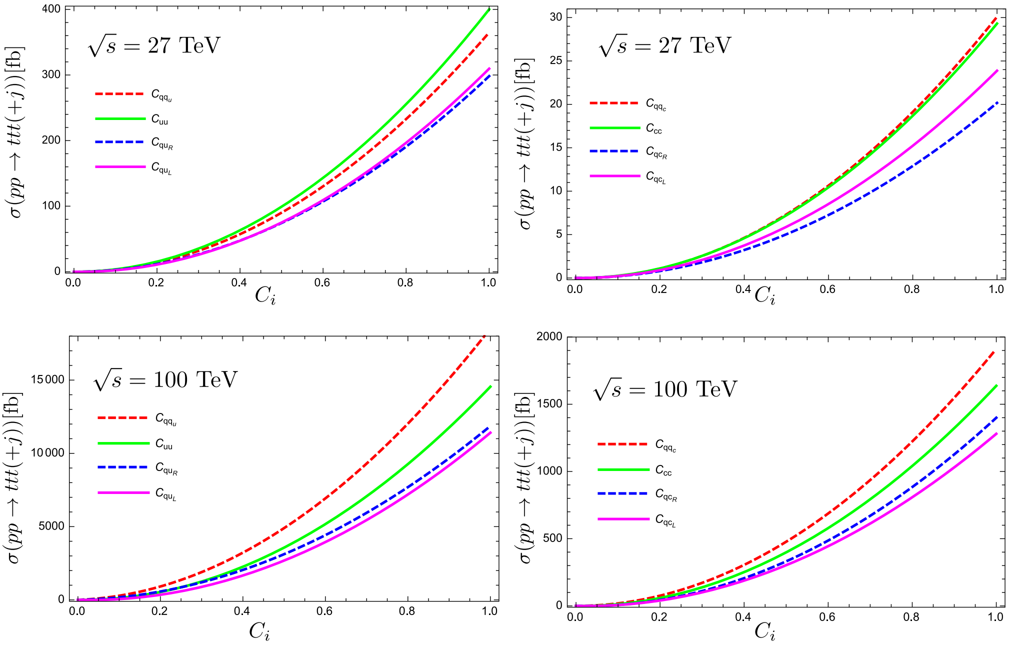

Fig. 2. The signal cross section including the branching ratios as a function of Wilson coefficients for $\Lambda = 1$ TeV after applying the preselection at the center of mass energy 27 TeV and 100 TeV.

Fig. 1 presents some representative Feynman diagrams of the signal process. The triple top and triple top in association with a jet production in presence of the four-fermion contact interactions are shown in the first row and second row, respectively. The effective Lagrangian of Eq. (3) is implemented in the FEYNRULES package [34] and the obtained UFO module [35] is inserted in the MADGRAPH 5 package [36] for generating the signal events.

We generate eight different signal samples corresponding to the eight different Wilson coefficients (Eq. (3)) to probe each of them separately. The signal cross section including the branching ratios as a function of different Wilson coefficients for the HE-LHC and the FCC-hh colliders at the center of mass energy 27 TeV and 100 TeV are depicted in Fig. 2. The plots for Wilson coefficients related to u-quark and c-quark are shown separately. As we expected, the cross section values corresponding to u-quark are around one order of magnitude larger than the ones related to c-quark due to the large parton distribution function (PDF) of the u-quark in the proton compared to the c-quark. In order to generate the signal events, we set $\Lambda = 1$ TeV and apply preselection cuts, $p_T \geq 10$ GeV and $|\eta| < 3$ on all decay products.

Considering our signal signature, a complete set of the main SM background processes are considered in our study which includes the $t\bar{t}Z$, $t\bar{t}W^{\pm}$, W^+W^-Z and four top quark production $tt\bar{t}\bar{t}$. We also add the SM triple top quark production to the background process. However, since the three top quarks cannot generate in the framework of the SM alone, we consider $ttt + j$ and $ttt + W$ as the SM triple top quark background. All the mentioned SM backgrounds with their decay products are listed below:

$$pp \to t\bar{t}Z \to 3\,\ell + 2\text{ b-jet} + 2\text{ light-jet} + \not{E}_T\,,$$
$$pp \to t\bar{t}W^{\pm} \to 2\,\ell + 2\text{ b-jet} + 2\text{ light-jet} + \not{E}_T\,,$$

$$pp \to W^+W^-Z \to 3\ \ell + 2\ \text{light-jet} + \not{E}_T\ ,$$
$$pp \to tt\bar{t}\bar{t} \to 2\ \ell + 4\ \text{b-jet} + 4\ \text{light-jet} + \not{E}_T\ ,$$
$$pp \to tt\bar{t}(t\bar{t}\bar{t}) + j \to 2\ \ell + 3\ \text{b-jet} + 3\ \text{light-jet} + \not{E}_T\ ,$$
$$pp \to tt\bar{t}(t\bar{t}\bar{t}) + W \to 2(3)\ \ell + 3\ \text{b-jet} + 4(2)\ \text{light-jet} + \not{E}_T\ .$$

In order to generate the signal and background samples, the MadGraph 5 package is used. The following SM inputs are used in all numerical calculation: $m_{\text{top}} = 173.3$ GeV, $m_Z = 91.187$ GeV, $\alpha_{ew} = 1/127.90$, and $\alpha_s = 0.1184$ [37]. We employ the leading order of the `NNPDF23L01` as the parton distribution function [38,39]. Also, the dynamical scale is used for renormalization and factorization scale. Some preselection cuts such as $p_T \geq 10$ GeV and $|\eta| < 3$ are applied on all objects in the final state at the generator level. The Pythia package [40] is used for parton showering and hadronization. To simulate the signal and backgrounds including up to one additional jet in the final state, we employ the MLM matching scheme to avoid double counting [41,42].

Furthermore, the Delphes package [43] is utilized to model the detector performance. We should note here that, for our HE-LHC analysis, we use the Delphes framework to perform a comprehensive high luminosity (HL) CMS detector response simulation. To this end, the HL-LHC detector card configuration available in the Delphes is used which includes the high configuration of the CMS detector [30,44]. For the case of FCC-hh projections, we use the default FCC detector card configuration implemented in Delphes [45]. Considering these configurations, the efficiency of b- and c-tagging and light-flavor quarks misidentifications rates are assumed to be the jet transverse momentum dependent (p_T) [27].

For selecting the event rate for all signal scenarios, we require to apply the following selection cuts:

- Cut (I): $n^\ell = 2\ell^{\pm\pm}$, $|\eta^\ell| < 2.5$, $p_T^\ell > 10$ GeV, $M_{\ell^\pm\ell^\pm} > 10$ GeV.
- Cut (II): $\not{E}_T > 30$ GeV.
- Cut (III): $n^{\text{jets}} \geq 5$ jets, $|\eta^{\text{jets}}| < 2.5$, $p_T^{\text{jets}} > 20$ GeV, $\Delta R(\ell, j_i) \geq 0.4$, $\Delta R(j_i, j_j) \geq 0.4$.
- Cut (IV): $n^{\text{b}-\text{jets}} \geq 3\ \text{b} - \text{jets}$,

where $\Delta R = \sqrt{(\Delta\phi)^2 + (\Delta\eta)^2}$. In order to suppress the contributions of SM backgrounds, we look at the different kinematic distributions to find a proper secondary cut. In Fig. 3, we present some selected distributions for the signal sample and all main background processes at the center of mass energy of 100 TeV. The signal sample is generated for the $C_{uu} = 1$ and $\Lambda = 1$ TeV. The distribution of cosine between the leading charged-lepton ($\ell^\pm$) and the leading b-jet, $\cos(\ell, b)$, and the distribution of cosine between two same-sign charged leptons, $\cos(\ell^\pm, \ell^\pm)$, are illustrated. The angular distance between the leading charged-lepton and the leading b-jet $\Delta R(\ell, b)$ and $H_T + \not{E}_T$ distribution are shown as well. Here, the definition of the H_T is the sum of all the leptons and jets p_T.

All the distributions are presented after applying all the selection cuts described above. The cut efficiency of W^+W^-Z background is around 10^{-5}, therefore the distribution of this background isn't shown in Fig. 3. From $H_T + \not{E}_T$ distribution, it is clear that the signal has more spread distribution which extends up to around 1 TeV. The $H_T + \not{E}_T$ distribution for all other signal scenario has the same behavior. In order to separate more signal from the background events, we could add another criterion to our selection cuts as follows,

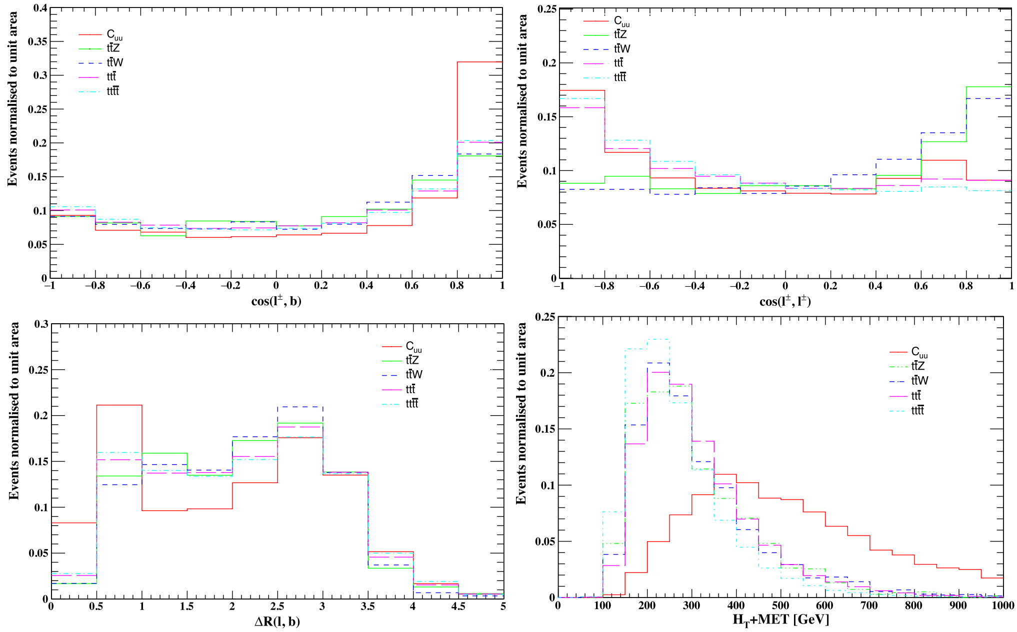

Fig. 3. The kinematic distributions of the triplet top (+jet) signal (for C_{uu} coupling and $\Lambda = 1$ TeV) and the main SM backgrounds, $t\bar{t}Z$, $t\bar{t}W$, SM three top ($t\bar{t}t$, $\bar{t}t\bar{t}$) and SM four top production ($t\bar{t}t\bar{t}$), at the center of mass energy of $\sqrt{s} = 100$ TeV.

- Cut (V): $H_T + \not{E}_T \geq 340$ GeV.

It can be seen from Fig. 2, for the different signal scenarios, we can write the dependence of the cross sections to the operator coefficients as follows,

$$\sigma = \sigma_0^i \times (\frac{C_i}{\Lambda^2})^2. \tag{4}$$

In Table 1, these values of σ_0^i for eight signal scenarios (different C_is) before and after the selection criteria are presented for the HE-LHC and FCC-hh colliders at the center of mass energy 27 TeV and 100 TeV. Moreover, the expected cross sections include the branching ratios for the relevant SM backgrounds are shown in Table 2 which are reported in the unit of fb. We should highlight here that the values in the first rows of two tables are reported after applying the preselection cuts.

It should be mentioned here that, we consider two other potential sources of background categories. The first category rises up from mismeasurement of the charge of leptons. The same-sign signature can be appeared in processes like $t\bar{t}$ dilepton channel, tW dilepton channel, and Drell-Yan, if the charge of a lepton is mismeasured and they can play the role of the background process. The efficiencies for these background processes are completely negligible after applying the secondary cuts, particularly when we require the cuts on the number of jets ($n^{\text{jets}} \geq 5$). The efficiency of whole background is less than 0.01%(0.1%) at center of mass energy of 27(100) TeV. Also, these efficiencies should multiply in the charge mismeasurement probability which is about $3.3 \pm 0.2 \times 10^{-4}$ for electron, whereas this value for muon is tiny [48]. As a result, the contributions from these backgrounds are rather small and safely could be neglected.

Table 1
The values for σ_0 (in the unit of fbTeV^4) including the branching ratios for eight signal scenarios, before and after the selection criteria for the HE-LHC and FCC-hh colliders.

$\sqrt{s}$ = 27 TeV (HE-LHC)	C_{qq_u}	C_{uu}	C_{qu_R}	C_{qu_L}	C_{qq_c}	C_{cc}	C_{qc_R}	C_{qc_L}
Preselection cuts	373.44	392.83	298.17	310.94	30.52	30.01	20.55	24.15
Cut (I)	75.18	86.89	75.80	79.43	7.61	8.92	6.08	7.11
Cut (II)	74.81	86.42	75.38	79.06	7.57	8.85	6.04	7.07
Cut (III)	49.43	51.15	48.16	51.75	4.84	5.13	3.75	4.54
Cut (IV)	19.25	16.96	18.97	19.13	1.94	1.71	1.45	1.67
Cut (V)	11.03	12.48	11.10	11.00	0.96	1.11	0.77	0.84
$\sqrt{s}$ = 100 TeV (FCC-hh)	C_{qq_u}	C_{uu}	C_{qu_R}	C_{qu_L}	C_{qq_c}	C_{cc}	C_{qc_R}	C_{qc_L}
Preselection cuts	17862.71	14379.80	12376.94	12957.84	1881.59	1649.85	1431.31	1403.15
Cut (I)	2147.37	1830.48	2322.97	2442.03	382.37	388.14	391.41	383.42
Cut (II)	2138.79	1820.91	2312.63	2432.19	380.58	386.02	389.47	381.53
Cut (III)	1768.59	1420.94	1882.59	1993.76	316.52	303.08	318.43	314.05
Cut (IV)	875.00	602.58	937.98	954.73	160.01	132.25	161.49	151.48
Cut (V)	567.05	481.43	616.99	611.22	95.39	97.98	98.58	91.65

Table 2
Cross section (in the unit of fb) including the branching ratios for the $t\bar{t}Z$, $t\bar{t}W$, WWZ, SM three top ($t\bar{t}t$, $\bar{t}t\bar{t}$) and SM four top production ($t\bar{t}t\bar{t}$), before and after the selection criteria, for the HE-LHC and FCC-hh colliders.

$\sqrt{s}$ = 27 TeV (HE-LHC)	$t\bar{t}Z$	$t\bar{t}W$	WWZ	SM ($t\bar{t}t$, $\bar{t}t\bar{t}$)	SM ($t\bar{t}t\bar{t}$)
Preselection cuts	33.92	17.45	3.03	0.188	0.940
Cut (I)	4.26	6.57	0.36	0.032	0.271
Cut (II)	3.62	5.90	0.28	0.029	0.251
Cut (III)	1.31	1.06	0.011	0.022	0.227
Cut (IV)	0.132	0.117	0.00003	0.009	0.121
Cut (V)	0.02	0.02	0.0	0.002	0.033
$\sqrt{s}$ = 100 TeV (FCC-hh)	$t\bar{t}Z$	$t\bar{t}W$	WWZ	SM ($t\bar{t}t$, $\bar{t}t\bar{t}$)	SM ($t\bar{t}t\bar{t}$)
Preselection cuts	343.44	73.16	12.45	2.83	15.18
Cut (I)	39.424	32.09	1.30	0.54	5.03
Cut (II)	33.23	28.96	1.01	0.50	4.68
Cut (III)	19.59	11.53	0.11	0.46	4.60
Cut (IV)	2.76	1.53	0.00056	0.25	3.27
Cut (V)	0.728	0.310	0.0	0.088	0.717

The second category comes from when a jet is misidentified as a lepton. Some example of this sort of background process are: (i) $W+$ jets events in which W decays leptonically and one of the jets is misidentified as a lepton; (ii) Semi-leptonic $t\bar{t}$ events in which the second leptons originated from misidentification of a jet; and (iii) the t-channel single top production in which top quark decay leptonically and one of the jets fakes the lepton. We found pretty small efficiencies for these backgrounds after imposing the secondary cuts. Hence we neglect the contributions of these two sources of backgrounds in our analysis.

4. Sensitivity estimation

This section presents the potential sensitivity of HE-LHC and FCC-hh colliders to probe the contact interactions. We demonstrate the upper limits on the Wilson coefficients of the four-

Table 3
Constraints at 95% CL on the Wilson coefficients ($C_i(1\ \text{TeV})^2/\Lambda^2$) of four-fermion operators at the center of mass energy of 27 TeV (HE-LHC) and 100 TeV (FCC-hh) with the integrated luminosity of 15 ab^{-1} and 30 ab^{-1}, respectively. We consider an overall systematic uncertainty of 0% and 10% on the signal efficiency and number of backgrounds At a time one of the coupling is considered in the analysis.

Wilson coefficient	HE-LHC, 15 ab^{-1}		FCC − hh, 30 ab^{-1}	
	$\delta = 0\%$	$\delta = 10\%$	$\delta = 0\%$	$\delta = 10\%$
C_{qqu}	[−0.042, 0.011]	[−0.044, 0.013]	[−0.018, 0.0017]	[−0.019, 0.0019]
C_{uu}	[−0.008, 0.047]	[−0.009, 0.048]	[−0.055, 0.0007]	[−0.056, 0.0008]
C_{qu_R}	[−0.020, 0.023]	[−0.021, 0.025]	[−0.003, 0.013]	[−0.003, 0.014]
C_{qu_L}	[−0.021, 0.022]	[−0.023, 0.024]	[−0.002, 0.011]	[−0.002, 0.012]
C_{qqc}	[−0.068, 0.078]	[−0.074, 0.084]	[−0.006, 0.028]	[−0.007, 0.029]
C_{cc}	[−0.067, 0.069]	[−0.073, 0.075]	[−0.007, 0.023]	[−0.008, 0.024]
C_{qc_R}	[−0.125, 0.057]	[−0.131, 0.064]	[−0.003, 0.044]	[−0.004, 0.045]
C_{qc_L}	[−0.059, 0.100]	[−0.065, 0.106]	[−0.003, 0.059]	[−0.003, 0.060]

fermion interactions involving three top quarks at 95% confidence level (CL) by analyzing triple top quarks (+jet) production. A Bayesian approach with a flat prior distribution is employed to estimate the upper limits. The probability of observing number of events is assumed to have a Poisson distribution [37],

$$L\,(n_{\text{obs}}, n_{\text{S}}, n_{\text{B}}) = \frac{(n_{\text{S}} + n_{\text{B}})^{n_{\text{obs}}}}{n_{\text{obs}}!} e^{-(n_{\text{S}}+n_{\text{B}})}, \tag{5}$$

here $n_{\text{S}} = \epsilon_{\text{S}} \times \mathcal{L} \times \sigma_{\text{S}}$ where ϵ_{S} and $\mathcal{L}$ are the efficiency of the signal and the integrated luminosity, respectively. The number of background events are given by $n_{\text{B}} = \epsilon_{\text{B}} \times \mathcal{L} \times \sigma_{\text{B}}$ that ϵ_{B} is the efficiency of the backgrounds. The upper limit at 95% CL on the number of signal events can be obtained using following formula:

$$\frac{95}{100} = \frac{\int_0^{n_{\text{limit}}} L\,(n_{\text{obs}}, n_{\text{S}}, n_{\text{B}})\, \mathrm{d}n_{\text{S}}}{\int_0^{\infty} L\,(n_{\text{obs}}, n_{\text{S}}, n_{\text{B}})\, \mathrm{d}n_{\text{S}}}. \tag{6}$$

In order to obtain the upper limit on the number of signal events, we assume that the observed number of events are in consistent with the expected number of background events. Then we translate this upper limit to the signal cross section and Wilson coefficients of four-fermion interaction. Table 3 presents the upper limits at 95% CL on the Wilson coefficients of four-fermion operators involving three top quarks at the center of mass energy 27 TeV and 100 TeV with the integrated luminosity of 15 ab^{-1} and 30 ab^{-1}, respectively. It worth mentioning that, at a time one of the couplings is considered in the analysis.

For finding the upper limits, we scale the production cross section of our main backgrounds to their next-to-leading (NLO) values. The NLO corrections to the $t\bar{t}Z$, $t\bar{t}W$ and $t\bar{t}t\bar{t}$ production can be found in Ref. [30] for the HE-LHC and Ref. [46,47] for FCC-hh. The cross sections for $t\bar{t}Z$, $t\bar{t}W$ and $t\bar{t}t\bar{t}$ are multiplied by the NLO K-factors of 1.2 (1.17), 1.6 (2.2) and 1.3 (1.2) at the HE-LHC (FCC-hh), respectively.

Furthermore for finding more realistic upper limits, the systematic uncertainties should be taken into account. The source of systematic uncertainties comes from factorization and renormalization scales, proton parton distribution function, top quark mass, luminosity measurements, etc. In this analysis, we consider an overall systematic uncertainty of 10% on the signal efficiency and the number of backgrounds. The obtained limits with considering 10% systematic error are

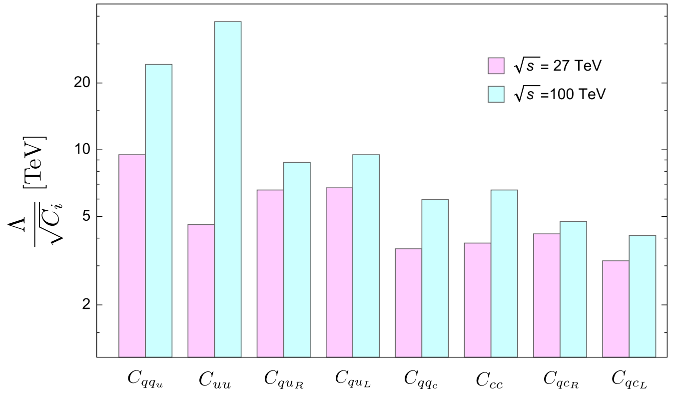

Fig. 4. The limits at 95% CL on $\Lambda/\sqrt{C_i}$ at the center of mass energy of 27 TeV (HE-LHC) and 100 TeV (FCC-hh) with the integrated luminosity of 15 ab^{-1} and 30 ab^{-1}, respectively.

shown in Table 3 as well. As it is clear from the table by considering the 10% systematic error, we have the weaker upper limits on the Wilson coefficients of effective operators. In Fig. 4, we present our bound at 95% CL on the $\Lambda/\sqrt{C_i}$ at HE-LHC and FCC-hh with the integrated luminosity of 15 ab^{-1} and 30 ab^{-1}, respectively.

As mentioned before, one can translate the upper limits on the Wilson coefficients to the parameters of the UV complete model. For instance, a model containing a new leptophobic gauge boson Z' associated with an abelian gauge symmetry U(1) with following interaction term can capture some of our contact operators at low energy [49],

$$\mathcal{L}^{Z'} \supset g_{FC}\bar{t}_R\gamma^\mu t_R Z'_\mu + \{g_{FV}\bar{u}_R\gamma^\mu t_R Z'_\mu + h.c.\}, \tag{7}$$

where g_{FC} and g_{FV} are flavor conserving and flavor violating couplings, respectively. After integrating the Z' out the obtained effective Lagrangian included flowing term:

$$\mathcal{L}^{Z'}_{\rm eff} \supset \frac{-g_{FC}g_{FV}}{2M^2_{Z'}}(\bar{t}_R\gamma^\mu t_R)(\bar{u}_R\gamma^\mu t_R) + h.c. \tag{8}$$

By comparing the effective Lagrangians in Eq. (3) and Eq. (8), it is found that $C_{uu} = -g_{FC}g_{FV}/2$ and $\Lambda = M_{Z'}$ at the tree level. As a result, we can find the allowed region for g_{FC} and g_{FV} couplings by using the upper limits on C_{uu}. Fig. 5 shows the allowed region for the Z' model at the center of mass energy 27 TeV with the integrated luminosity of 15 ab^{-1}. Since we need to be sure about the validity of the EFT approach, the assumed Z' masses should be sufficiently larger than the relevant energies and momenta of our processes. As result, we choose the $M_{Z'} = 4$ TeV and $M_{Z'} = 5$ TeV benchmarks to find the limits on Z' couplings. If consider the same value for the flavor conserving and flavor violating couplings ($g = g_{FC} = g_{FV}$), the upper limits at 95% CL is found to be $|g| < 1.2$ (1.5) for $M_{Z'} = 4$ (5) TeV.

5. Summary

The Standard Model Effective Field Theory (SMEFT) is a model-independent approach to search for new physics in the colliders. The SMEFT Lagrangian consists of higher-order operators only containing the SM degrees of freedom and respecting the Lorentz and the SM gauge symmetry. Among leading corrections to the SM Lagrangian, the four-fermion interactions can

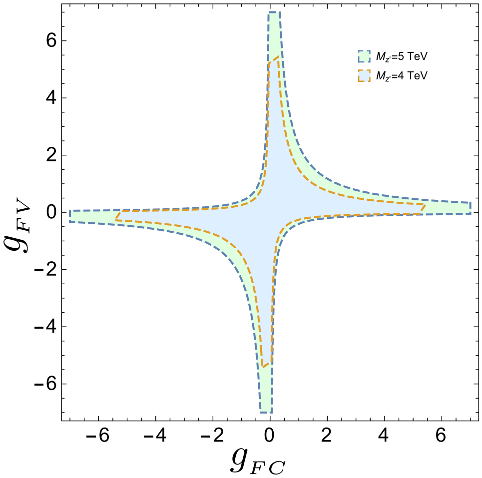

Fig. 5. The allowed region (at 95% CL) for Z' parameter space at the center of mass energy 27 TeV with the integrated luminosity of 15 ab^{-1} for $M_{Z'} = 4$ TeV and $M_{Z'} = 5$ TeV.

be originated at the tree level in the UV completion model therefore they can have large Wilson coefficients.

In this paper, we examine the sensitivity potential of the future high-energy proton-proton colliders to probe the four-fermion contact interaction involving three top quarks. We study the three top quarks and three top quarks+jet productions in the future hadron colliders to explore the three top-one light quark operators. A detailed analysis considering the full set of background processes and the real detector simulation is performed. We find the upper limits at the 95% CL on the Wilson coefficients for the high energy LHC (HE-LHC) and the Future Circular Collider (FCC-hh) colliders at the center of mass energy of 27 TeV and 100 TeV with the integrated luminosity of 15 ab^{-1} and 30 ab^{-1}, respectively. Furthermore, we consider a UV completion model, a leptophobic Z' boson associated with an abelian gauge symmetry U(1) and by matching we find the model's allowed region for different Z' mass values.

CRediT authorship contribution statement

Sara Khatibi: Idea, Disscution, Writing, Editing. **Hamzeh Khanpour:** Analysis, Disscution, Reviewing.

Declaration of competing interest

The authors declare that they have no known competing financial interests or personal relationships that could have appeared to influence the work reported in this paper.

Acknowledgements

Authors are thankful to Mojtaba Mohammadi Najafabadi for valuable comments on the manuscript and many helpful discussions. SK thanks also Mikael Chala for useful discussions. HK thanks School of Particles and Accelerators, Institute for Research in Fundamental Sciences

(IPM) and University of Science and Technology of Mazandaran for financial support of this research.

References

[1] I. Brivio, M. Trott, The standard model as an effective field theory, Phys. Rep. 793 (2019) 1–98, arXiv:1706.08945.
[2] B. Grzadkowski, M. Iskrzynski, M. Misiak, J. Rosiek, Dimension-six terms in the standard model Lagrangian, J. High Energy Phys. 10 (2010) 085, arXiv:1008.4884.
[3] J. de Blas, J. Criado, M. Perez-Victoria, J. Santiago, Effective description of general extensions of the Standard Model: the complete tree-level dictionary, J. High Energy Phys. 03 (2018) 109, arXiv:1711.10391.
[4] O. Domenech, A. Pomarol, J. Serra, Probing the SM with Dijets at the LHC, Phys. Rev. D 85 (2012) 074030, arXiv:1201.6510.
[5] F. del Aguila, M. Chala, J. Santiago, Y. Yamamoto, Collider limits on leptophilic interactions, J. High Energy Phys. 03 (2015) 059, arXiv:1411.7394.
[6] A. Falkowski, K. Mimouni, Model independent constraints on four-lepton operators, J. High Energy Phys. 02 (2016) 086, arXiv:1511.07434.
[7] J. D'Hondt, A. Mariotti, K. Mimasu, S. Moortgat, C. Zhang, Learning to pinpoint effective operators at the LHC: a study of the $t\bar{t}b\bar{b}$ signature, J. High Energy Phys. 11 (2018) 131, arXiv:1807.02130.
[8] A. Buckley, C. Englert, J. Ferrando, D.J. Miller, L. Moore, M. Russell, C.D. White, Global fit of top quark effective theory to data, Phys. Rev. D 92 (9) (2015) 091501, arXiv:1506.08845.
[9] C. Degrande, J.-M. Gerard, C. Grojean, F. Maltoni, G. Servant, Non-resonant new physics in top pair production at hadron colliders, J. High Energy Phys. 03 (2011) 125, arXiv:1010.6304.
[10] CMS Collaboration, Projections of sensitivities for tttt, production at HL-LHC and HE-LHC.
[11] G. Banelli, E. Salvioni, J. Serra, T. Theil, A. Weiler, The present and future of four tops, J. High Energy Phys. 02 (2021) 043, arXiv:2010.05915.
[12] ATLAS Collaboration, G. Aad, et al., Analysis of events with b-jets and a pair of leptons of the same charge in pp collisions at $\sqrt{s} = 8$ TeV with the ATLAS detector, J. High Energy Phys. 10 (2015) 150, arXiv:1504.04605.
[13] ATLAS Collaboration, G. Aad, et al., Search for production of vector-like quark pairs and of four top quarks in the lepton-plus-jets final state in pp collisions at $\sqrt{s} = 8$ TeV with the ATLAS detector, J. High Energy Phys. 08 (2015) 105, arXiv:1505.04306.
[14] J. Aguilar-Saavedra, Effective four-fermion operators in top physics: a roadmap, Nucl. Phys. B 843 (2011) 638–672, arXiv:1008.3562, Erratum: Nucl. Phys. B 851 (2011) 443–444.
[15] I. Brivio, S. Bruggisser, F. Maltoni, R. Moutafis, T. Plehn, E. Vryonidou, S. Westhoff, C. Zhang, O new physics, where art thou? A global search in the top sector, J. High Energy Phys. 02 (2020) 131, arXiv:1910.03606.
[16] N.P. Hartland, F. Maltoni, E.R. Nocera, J. Rojo, E. Slade, E. Vryonidou, C. Zhang, A Monte Carlo global analysis of the Standard Model effective field theory: the top quark sector, J. High Energy Phys. 04 (2019) 100, arXiv:1901.05965.
[17] J. Aguilar-Saavedra, C. Degrande, S. Khatibi, Single top polarisation as a window to new physics, Phys. Lett. B 769 (2017) 498–502, arXiv:1701.05900.
[18] P.J. Fox, Z. Ligeti, M. Papucci, G. Perez, M.D. Schwartz, Deciphering top flavor violation at the LHC with B factories, Phys. Rev. D 78 (2008) 054008, arXiv:0704.1482.
[19] G. Durieux, F. Maltoni, C. Zhang, Global approach to top-quark flavor-changing interactions, Phys. Rev. D 91 (7) (2015) 074017, arXiv:1412.7166.
[20] M. Chala, J. Santiago, M. Spannowsky, Constraining four-fermion operators using rare top decays, J. High Energy Phys. 04 (2019) 014, arXiv:1809.09624.
[21] J. de Blas, M. Chala, M. Perez-Victoria, J. Santiago, Observable effects of general new scalar particles, J. High Energy Phys. 04 (2015) 078, arXiv:1412.8480.
[22] V. Barger, W.-Y. Keung, B. Yencho, Triple-top signal of new physics at the LHC, Phys. Lett. B 687 (2010) 70–74, arXiv:1001.0221.
[23] W.-S. Hou, M. Kohda, T. Modak, Implications of four-top and top-pair studies on triple-top production, Phys. Lett. B 798 (2019) 134953, arXiv:1906.09703.
[24] M. Kohda, T. Modak, W.-S. Hou, Searching for new scalar bosons via triple-top signature in $cg \to tS^0 \to tt\bar{t}$, Phys. Lett. B 776 (2018) 379–384, arXiv:1710.07260.
[25] C. Han, N. Liu, L. Wu, J.M. Yang, Probing topcolor-assisted technicolor from top charge asymmetry and triple-top production at the LHC, Phys. Lett. B 714 (2012) 295–300, arXiv:1203.2321.

[26] M. Malekhosseini, M. Ghominejad, H. Khanpour, M. Mohammadi Najafabadi, Constraining top quark flavor violation and dipole moments through three and four-top quark productions at the LHC, Phys. Rev. D 98 (9) (2018) 095001, arXiv:1804.05598.
[27] H. Khanpour, Probing top quark FCNC couplings in the triple-top signal at the high energy LHC and future circular collider, Nucl. Phys. B 958 (2020) 115141, arXiv:1909.03998.
[28] Q.-H. Cao, S.-L. Chen, Y. Liu, X.-P. Wang, What can we learn from triple top-quark production?, Phys. Rev. D 100 (5) (2019) 055035, arXiv:1901.04643.
[29] C.-R. Chen, Searching for new physics with triple-top signal at the LHC, Phys. Lett. B 736 (2014) 321–324.
[30] P. Azzi, et al., Report from working group 1: Standard Model physics at the HL-LHC and HE-LHC, vol. 7, pp. 1–220. 12, 2019, arXiv:1902.04070.
[31] M. Cepeda, et al., Report from working group 2: Higgs physics at the HL-LHC and HE-LHC, vol. 7, pp. 221–584. 12, 2019, arXiv:1902.00134.
[32] FCC Collaboration, A. Abada, et al., FCC-hh: the hadron collider: future circular collider conceptual design report volume 3, Eur. Phys. J. Spec. Top. 228 (4) (2019) 755–1107.
[33] D. Barducci, et al., Interpreting top-quark LHC measurements in the standard-model effective field theory, arXiv:1802.07237.
[34] A. Alloul, N.D. Christensen, C. Degrande, C. Duhr, B. Fuks, FeynRules 2.0 - a complete toolbox for tree-level phenomenology, Comput. Phys. Commun. 185 (2014) 2250–2300, arXiv:1310.1921.
[35] C. Degrande, C. Duhr, B. Fuks, D. Grellscheid, O. Mattelaer, T. Reiter, UFO - the universal FeynRules output, Comput. Phys. Commun. 183 (2012) 1201–1214, arXiv:1108.2040.
[36] J. Alwall, R. Frederix, S. Frixione, V. Hirschi, F. Maltoni, O. Mattelaer, H.S. Shao, T. Stelzer, P. Torrielli, M. Zaro, The automated computation of tree-level and next-to-leading order differential cross sections, and their matching to parton shower simulations, J. High Energy Phys. 07 (2014) 079, arXiv:1405.0301.
[37] Particle Data Group Collaboration, M. Tanabashi, et al., Review of particle physics, Phys. Rev. D 98 (3) (2018) 030001.
[38] R.D. Ball, et al., Parton distributions with LHC data, Nucl. Phys. B 867 (2013) 244–289, arXiv:1207.1303.
[39] NNPDF Collaboration, R.D. Ball, et al., Parton distributions from high-precision collider data, Eur. Phys. J. C 77 (10) (2017) 663, arXiv:1706.00428.
[40] P. Skands, S. Carrazza, J. Rojo, Tuning PYTHIA 8.1: the Monash 2013 tune, Eur. Phys. J. C 74 (8) (2014) 3024, arXiv:1404.5630.
[41] M.L. Mangano, M. Moretti, F. Piccinini, M. Treccani, Matching matrix elements and shower evolution for top-quark production in hadronic collisions, J. High Energy Phys. 01 (2007) 013, arXiv:hep-ph/0611129.
[42] R. Frederix, S. Frixione, Merging meets matching in MC@NLO, J. High Energy Phys. 12 (2012) 061, arXiv:1209.6215.
[43] DELPHES 3 Collaboration, J. de Favereau, C. Delaere, P. Demin, A. Giammanco, V. Lemaitre, A. Mertens, M. Selvaggi, DELPHES 3, a modular framework for fast simulation of a generic collider experiment, J. High Energy Phys. 02 (2014) 057, arXiv:1307.6346.
[44] A. Cerri, et al., Report from working group 4: opportunities in flavour physics at the HL-LHC and HE-LHC, CERN Yellow Rep. Monogr. 7 (2019) 867–1158, arXiv:1812.07638.
[45] K. Oyulmaz, A. Senol, H. Denizli, O. Cakir, Top quark anomalous FCNC production via tqg couplings at FCC-hh, Phys. Rev. D 99 (11) (2019) 115023, arXiv:1902.03037.
[46] M.L. Mangano, et al., Physics at a 100 TeV pp collider: Standard Model processes, arXiv:1607.01831.
[47] F. Maltoni, D. Pagani, I. Tsinikos, Associated production of a top-quark pair with vector bosons at NLO in QCD: impact on $t\bar{t}$H searches at the LHC, J. High Energy Phys. 02 (2016) 113, arXiv:1507.05640.
[48] CMS Collaboration, S. Chatrchyan, et al., Search for heavy Majorana neutrinos in $\mu^{\pm}\mu^{\pm}+$ Jets and $e^{\pm}e^{\pm}+$ Jets events in pp collisions at $\sqrt{s}=7$ TeV, Phys. Lett. B 717 (2012) 109–128, arXiv:1207.6079.
[49] S. Jung, H. Murayama, A. Pierce, J.D. Wells, Top quark forward-backward asymmetry from new t-channel physics, Phys. Rev. D 81 (2010) 015004, arXiv:0907.4112.